Received: 27 May 2024 | Revised: 9 September 2024 | Accepted: 12 September 2024

DOI: 10.1002/rcm.9921

RESEARCH ARTICLE

Rapid Communications in Mass Spectrometry WILEY

Triple-oxygen isotopes of stony micrometeorites by secondary ion mass spectrometry (SIMS): Olivine, basaltic glass and iron oxide matrix effects for sensitive high-mass resolution ion microprobe-stable isotope (SHRIMP-SI)

Seann J. McKibbin[1,2,3,4] | Janaína N. Ávila[3,5] | Trevor R. Ireland[3,6] | Matthias Van Ginneken[1,7,8,9] | Bastien Soens[1] | Flore Van Maldeghem[1] | Matthew Huber[10] | Leonardo Baeza[3] | Aditya Patkar[3] | Frank Vanhaecke[11] | Vinciane Debaille[7] | Philippe Claeys[1] | Steven Goderis[1]

[1]Analytical, Environmental and Geo-Chemistry, Vrije Universiteit Brussel, Brussels, Belgium

[2]Geowissenschaftliches Zentrum, Abteilung Isotopengeologie, Georg-August-Universität Göttingen, Göttingen, Germany

[3]Research School of Earth Sciences, Australian National University, Acton, ACT, Australia

[4]Earth Atmosphere and Environment, Monash University, Clayton, Victoria, Australia

[5]Griffith Centre for Social and Cultural Research, Griffith University, Nathan, Queensland, Australia

[6]School of Earth and Environmental Sciences, The University of Queensland, St Lucia, Queensland, Australia

[7]Laboratoire G-Time, Université Libre de Bruxelles, Brussels, Belgium

[8]Belgian Geological Survey, Royal Belgian Institute of Natural Sciences, Brussels, Belgium

[9]Center for Astrophysics and Planetary Science, School of Physical Sciences, Ingram Building, University of Kent, Canterbury, UK

[10]Planetary Science Institute, Tucson, Arizona, USA

[11]Department of Chemistry, Universiteit Gent, Ghent, Belgium

Correspondence
Seann J. McKibbin, Earth Atmosphere and Environment, Monash University, 9 Rainforest Walk, Clayton, VIC 3800, Australia.
Email: seann.mckibbin@gmail.com

Funding information
Belgian Federal Science Policy Office; Fonds De La Recherche Scientifique - FNRS; Alexander von Humboldt-Stiftung; Fonds Wetenschappelijk Onderzoek; FVM, the Interuniversity Attraction Poles Program (IUAP) Planet Topers and the BRAIN-be BAMM, Grant/Award Number: 11C2520N; Belgian Science Policy Office and the FWO/FNRS Excellence of Science, Grant/Award Number: 30442502

Rationale: Micrometeorites are extraterrestrial particles smaller than ~2 mm in diameter, most of which melted during atmospheric entry and crystallised or quenched to form 'cosmic spherules'. Their parentage among meteorite groups can be inferred from triple-oxygen isotope compositions, for example, by secondary ion mass spectrometry (SIMS). This method uses sample efficiently, preserving spherules for other investigations. While SIMS precisions are improving steadily, application requires assumptions about instrumental mass fractionation, which is controlled by sample chemistry and mineralogy (matrix effects).

Methods: We have developed a generic SIMS method using sensitive high-mass resolution ion micro probe-stable isotope (SHRIMP-SI) that can be applied to finely crystalline igneous textures as in cosmic spherules. We correct for oxygen isotope matrix effects using the bulk chemistry of samples obtained by laser ablation inductively coupled plasma mass spectrometry (LA-ICP-MS) and model bulk chemical

compositions as three-component mixtures of olivine, basaltic glass and Fe-oxide (magnetite), finding a unique matrix correction for each target.

Results: Our first results for cosmic spherules from East Antarctica compare favourably with established micrometeorite groups defined by precise and accurate but consumptive bulk oxygen isotope methods. The Fe-oxide content of each spherule is the main control on magnitude of oxygen isotope ratio bias, with effects on $\delta^{18}O$ up to ~6‰. Our main peak in compositions closely coincides with so-called 'Group 1' objects identified by consumptive methods.

Conclusions: The magnitude of SIMS matrix effects we find is similar to the previous intraspherule variations, which are now the limiting factor in understanding their compositions. The matrix effect for each spherule should be assessed quantitatively and individually, especially addressing Fe-oxide content. We expect micrometeorite triple-oxygen isotope compositions obtained by SIMS to converge on the main clusters (Groups 1 to 4) after correction firstly for magnetite content and secondarily for other phases (e.g., basaltic glass) in each target.

1 | INTRODUCTION

The majority of asteroidal material delivered to the Earth occurs as fine grains referred to as micrometeorites. These are small particles, by definition <2 mm diameter and typically smaller than 1 mm diameter. They are usually modified by their passage through the atmosphere, often to high degrees of partial melting, forming 'cosmic spherules'. Despite fractionation due to evaporation and mixing with atmospheric oxygen, their provenances can be found by comparison of their oxygen isotopic compositions with those of larger meteorites.[1–3] Currently, the highest precision oxygen isotope measurements of such materials are made by bulk, consumptive methods such as laser fluorination-assisted isotope ratio mass spectrometry (LF-IRMS[2]). Because this approach generally consumes an entire cosmic spherule (requiring ~1 mg of sample mass), it can only leave other mineralogical and petrological characteristics to be inferred by indirect methods, such as magnetic characterisation, X-ray computed microtomography or X-ray diffraction.[2,4] Alternatively, in situ measurements of the oxygen isotope compositions of cosmic spherules can be obtained by secondary ion mass spectrometry (SIMS), which has a lower precision but is nearly nondestructive (consuming less than ~10 ng of sample), preserving nearly the entire sample for further chemical investigation.[1,5] Such an approach is useful because variations in oxygen isotope ratios among cosmic spherules are rather large, and substantial improvements to analytical precision have been made in recent years.[6–9] Additionally, because SIMS enables preservation of sample early in an analytical campaign, it allows other types of in situ analyses to be conducted in parallel or during final consumption of the spherule in ambitious, high-precision ultra-trace element or isotope work (e.g., osmium).

In many previous SIMS studies of cosmic spherules and other geological materials, ionisation behaviour has often been approached quantitatively by various approximations. Among the most important metrics is instrumental mass fractionation (IMF) on an isotope ratio, which describes bias generated by a detector with respect to the true value in a sample. In SIMS, oxygen isotope IMF varies as a function of many variables including mineralogy and chemistry of the sample, and it is well understood only for a limited number of materials such as olivine. Over the years, research focus on such materials has often been driven simply by their widespread availability, such as magnesian mantle-derived olivine from San Carlos, Arizona, which is a commonly used primary SIMS standard (~Fo_{90}, where forsterite and fayalite components are given by $Fo_{\#}$ defined as $100 \times Mg/[Mg + Fe]$ on a molar basis). Some studies of micrometeorites have therefore focussed on determining accurate oxygen isotope compositions for relict and neocrystallised olivine.[1,6,7] However, many micrometeorites are finely crystalline, multiphase cosmic spherules in which phase-specific fractionation behaviour or 'matrix effects' are a significant source of uncertainty in analysis. At recently reported precisions for oxygen isotope ratios achieved by state-of-the-art methods (standard deviation of replicates frequently ~0.1 per mille; ‰), variation in IMF is routinely resolved as a function of composition for olivine[10,11] and for other phases such as glass or nonsilicate oxides.[12,13] Because of these matrix effects, previous studies that used SIMS to investigate finely crystalline cosmic spherules, and especially barred olivine or cryptocrystalline spherules in which multiphase sampling necessarily occurs, made no specific attempt at corrections for such samples.[5,9,14,15]

The lack of knowledge about possible bias in oxygen isotope compositions as well as of the elemental chemistry of particles (especially during application of LF-IRMS) make it difficult to correlate textural classes, volatile element evaporation and fractionation of oxygen isotopes during melting in the atmosphere. Among larger micrometeorites, there is a tendency for barred olivine cosmic

spherules to be related to carbonaceous chondrites and porphyritic olivine cosmic spherules to be related to ordinary chondrites,[16] but this leaves ambiguity in the relationship between texture, chemistry and oxygen isotope ratios, while the petrogenesis of other micrometeorite types is also relatively unexplored. Here, we take advantage of improved precisions achievable by SIMS and have developed a streamlined methodology for accurate in situ triple oxygen isotope analysis of finely crystalline micrometeorites, that is, a method applicable to most cosmic spherules. The major and minor element compositions, in this case obtained by laser ablation inductively coupled plasma mass spectrometry (LA-ICP-MS), are used in matrix effect corrections to SIMS oxygen isotope measurements made by sensitive high-mass resolution ion micro probe-stable isotope (SHRIMP-SI).[17] With this method, we are able to constrain the degree of isotopic fractionation in atmospheric melts and compare our dataset to other Solar System objects to identify what natural sampling biases on micrometeorite populations occur relative to other materials.

2 | METHODS

2.1 | Sample collection and preparation

Our study focusses on cosmic spherules separated from detritus collected in 2012 at Widerøefjellet (Mt. Widerøe, at ~2755 m a.s.l.; S72°8′41″, E23°16′41″) in the Sør Rondane Mountains, East Antarctica. Details on this collection and campaign are summarised previously.[4] Particles of interest were retrieved from two sedimentary samples (WF1 and WF2A) collected within an area ~100 m^2. These bulk sedimentary deposits were wet-sieved into six size fractions to remove excess silt and clay particles (>2000, 2000–800, 800–400, 400–200, 200–125 and <125 μm). Unlike the deposits picked in the previous study, magnetic particles were extracted from the respective size fractions using a simple Nd hand magnet. This step was performed to concentrate micrometeorites since the majority (>60%) of cosmic dust contains magnetite as a result of oxidative processes during atmospheric entry.[18] Micrometeorites from each of the

TABLE 1 Sample selection from the Widerøfjellet 1 (WF1) and 2A (WF2A) sedimentary deposits; with LA-ICP-MS major oxide compositions (wt.%); idealised proportions of Fo_{100}, basaltic and magnetite components; and weighted matrix effect for each micrometeorite.

Locality	WF1							WF2A			
Sample	−1	−2	−3	−4	−9	−11	−16	−18	−2	−8	−20
Type	Cc	BO	BO/cc	BO/cc	Cc	BO/cc	BO	Cc	BO/cc	BO	BO
Long axis (μm)	227	205	186	229	210	172	168	176	223	212	184
Short axis (μm)	176	188	176	190	200	157	158	175	216	198	174
Size (μm)	192	193	180	202	203	162	161	175	219	203	177
Weathering grade	0a	0a	1a	0a	0a	0a	2a	1a	0a	0a	0a
TiO_2	0.11	0.1	0.11	0.09	0.11	0.11	0.25	0.16	0.09	0.15	0.08
SiO_2	39.65	36.06	31.47	41.37	36.34	30.33	29.69	45.54	34.2	41.38	35.71
Al_2O_3	2.18	1.85	2.29	2.24	2.22	2.97	11.04	2.44	1.38	3.58	1.51
Cr_2O_3	0.06	0.7	0.35	0.17	0.58	0.01	0.51	0.35	0.19	0.06	0.27
FeO	27.07	35.43	37.05	26.31	34.49	38	33.36	19.72	26.58	25.17	30.47
NiO	0	1.1	0.83	0.06	0.97	0.07	0.65	0.7	0.01	0.97	0.19
MnO	0.42	0.3	0.23	0.22	0.26	0.37	0.29	0.18	0.22	0.21	0.49
MgO	28.5	21.15	26.29	28.77	22.89	26.25	20.56	28.53	36.15	25.78	30.07
CaO	2.08	3.65	1.27	0.9	2.62	1.75	1.92	1.7	1.17	2.69	0.72
Na_2O			0.05			0.02	0.59	0.15	0.05	0.02	0.12
K_2O			0.03			0.02	1.05	0.59	0.01	0.01	0.08
P_2O_5	0	0.26	0.16	0.01	0.08	0.02	0.34	0.21	0.08	0.06	0.12
Sum	100.05	100.58	100.13	100.14	100.54	99.91	100.25	100.26	100.15	100.08	99.83
% Fo_{100}	60.5	40.5	62	59.7	46	63	43.6	54.4	88.3	50.1	69.4
% basalt	20.2	33.6	5.5	23.8	28.9	2.6	17.8	34.9	−15.6	32.8	5.5
% magnetite	15.5	19.7	27.5	14	19.9	29	21.5	6	23.4	11.1	21.8
% other oxides	3.8	6.2	5	2.5	5.2	5.4	17.2	4.7	3.9	6	3.3
Matrix $Effect_{3\text{-comp.}}$	−3.57	−4.70	−6.28	−3.21	−4.67	−6.63	−5.71	−1.52	−5.19	−2.71	−4.90
Std. err.	0.30	0.42	0.45	0.29	0.40	0.47	0.45	0.20	0.31	0.28	0.35

*Note:*The weighted matrix effect is used in correction of $\delta^{18}O_{SC}$ to $\delta^{18}O_{3\text{-comp.}}$ (see Table 2), calculated from instrumental mass fractionation and matrix effect characteristics for each phase (see Table 3).

Abbreviation: LA-ICP-MS, laser ablation inductively coupled plasma mass spectrometry.

sedimentary samples were subsequently extracted from the 400- to 200-μm and 200- to 125-μm size fractions and embedded in their own epoxy resin mounts for analysis. Mounts were prepared for analysis by scanning electron microscope-energy dispersive spectrometry (SEM-EDS). The latter was carried out with a JEOL JSM IT-300 instrument at the Department of Chemistry (Vrije Universiteit Brussel) and used to measure particle dimensions and obtain a semiquantitative, geochemical composition of the particle selection. An overview of the sample selection is provided in Table 1. All samples fall into the barred olivine (BO) or cryptocrystalline (Cc) textural classes or are intermediate to those groups (BO/Cc) following the established classification scheme.[19] The size of each particle was measured from the polished section with SEM-EDS, and the average size was calculated assuming that the shape of cosmic spherules approximates an ellipsoid where a > b = c. The weathering grade indicates the extent of weathering experienced for each individual particle following the established classification scheme.[20]

2.2 | Secondary ionisation mass spectrometry

We used SHRIMP-SI to conduct SIMS analyses on cosmic spherules cast into epoxy mounts with their interiors exposed in polished sections (Figure 1). Samples were coated with aluminium and microbeam sampling was performed using a Cs^+ primary ion beam at a current of ~4 nA impacting the target at 15 keV. The spot size for all analyses was ~30 μm in average diameter, and two analyses were typically made in each spherule. Sputtering of each analytical spot was undertaken for 60 to 120 s to clean the surface and equilibrate the beam and sample by saturating with Cs before analysis. During this time, the electrometer backgrounds were measured, and the oxygen isotopic composition of the secondary ion beam was allowed to stabilise. The electron-induced secondary ion emission (EISIE) was measured before and after each analysis.[13] The mass resolution required for measuring ^{18}O is ~2300[13], while for the least abundant isotope ^{17}O, the required mass resolution is somewhat higher, at ~5000.[21] Secondary beam $^{16}O^-$ and $^{18}O^-$ ions were collected simultaneously by Faraday cups with electrometers using 10^{11} Ω input feedback resistors (iFlex) in current mode running at 50 and 5 V, respectively, while $^{17}O^-$ ions were collected by feedback capacitor (22 pF) in charge mode running at 10 V.

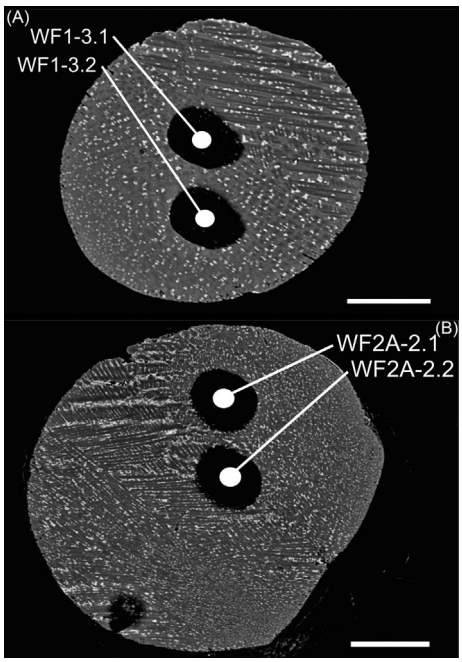

FIGURE 1 Backscatter electron (BSE) images of polished micrometeorite sections. The large, semispherical holes are sensitive high-mass resolution ion micro probe (SHRIMP) ablation pits. Scale bar is 50 μm. (A) Predominantly barred olivine texture in particle WF1-3. (B) Mixed barred olivine – cryptocrystalline texture in particle WF2A-2. Due to its intermediate texture, the particle was labelled accordingly

Although isotope ratios can be expressed absolutely by $^{17}O/^{16}O$ and $^{18}O/^{16}O$, they are frequently expressed in δ notation[22] relative to a reference composition. For oxygen, the major isotope ratio $\delta^{18}O$ is defined (here in per mille; ‰) as

$$\left[\left(^{18}O/^{16}O_{Sample}\right)/\left(^{18}O/^{16}O_{Reference}\right)-1\right]\times 1000$$

where the reference composition is that of a material with an assumed or known composition. For oxygen isotope work, it is typically reported relative to the composition of Standard Mean Ocean Water (SMOW)[23,24] or more recently Vienna Standard Mean Ocean Water (VSMOW).[25,26] The additional isotope ratio $\delta^{17}O$ is similarly defined as

$$\left[\left(^{17}O/^{16}O_{Sample}\right)/\left(^{17}O/^{16}O_{Reference}\right)-1\right]\times 1000$$

which in meteoritics has been important in distinguishing isotopically unique nebular or planetary sources.[27] Small variations in $\delta^{17}O$ with respect to $\delta^{18}O$ can be indicated by deviation of samples from a reference line[28]:

$$\Delta^{17}O=\delta^{17}O-\lambda\times\delta^{18}O$$

with a value of 0.52 commonly selected for λ to approximate mass-dependent fractionation behaviour.[29]

In time-resolved mass spectrometric data, 'internal' errors can be calculated as the standard deviation of the scans in each analysis, divided by the square root of the number of scans,[30] and we present this metric for our data in Table 2. Use of a scan-by-scan evaluation for $\Delta^{17}O$ produces uncertainties similar to or smaller than $\delta^{18}O$ and $\delta^{17}O$ through removal of variation caused by the correlated component of IMF.[5,31] To control for IMF, we frequently analysed San Carlos olivine and used it as our primary standard, like most other SIMS studies of the triple-oxygen isotopic compositions of cosmic spherules. Previously, high-precision LF-IRMS studies have resolved variations in oxygen isotope compositions for certain batches of San Carlos olivine at the level of ~0.3‰.[2] However, more recent LF-IRMS

TABLE 2 Micrometeorite triple-oxygen isotope SHRIMP-SI data, normalised to San Carlos olivine and with 3-component matrix correction

Sample	$\delta^{17}O_{SC}$	Int. err.	Ext. err.	$\delta^{18}O_{SC}$	Int. err.	Ext. err.	$\delta^{17}O_{3\text{-comp.}}$	Std. err.	$\delta^{18}O_{3\text{-comp.}}$	Std. err.	$\Delta^{17}O$	Int. err.	Ext. err.
WF1–1.1	10.90	0.11	0.30	23.99	0.04	0.12	12.78	0.34	27.66	0.32	−1.60	0.14	0.31
WF1–1.2	10.75	0.12	0.30	23.65	0.04	0.12	12.63	0.34	27.32	0.32	−1.57	0.16	0.32
WF1–2.1	12.88	0.10	0.29	28.99	0.06	0.12	15.36	0.37	33.84	0.44	−2.24	0.09	0.29
WF1–2.2	12.30	0.11	0.30	28.55	0.04	0.12	14.77	0.37	33.39	0.44	−2.59	0.16	0.32
WF1–3.1	11.67	0.13	0.30	26.20	0.05	0.12	14.98	0.38	32.67	0.46	−2.01	0.25	0.38
WF1–3.2	11.32	0.11	0.30	25.70	0.04	0.12	14.63	0.38	32.16	0.46	−2.09	0.18	0.33
WF1–4.1	14.11	0.11	0.29	30.67	0.04	0.12	15.80	0.33	33.98	0.31	−1.87	0.11	0.30
WF1–4.2	11.89	0.10	0.29	26.77	0.04	0.12	13.58	0.33	30.07	0.31	−2.06	0.10	0.30
WF1–9.1	12.16	0.11	0.29	29.72	0.05	0.12	14.63	0.36	34.54	0.42	−3.33	0.34	0.44
WF1–9.2	12.13	0.10	0.29	28.47	0.04	0.12	14.59	0.36	33.29	0.42	−2.72	0.10	0.30
WF1–11.1	14.63	0.10	0.29	23.21	0.05	0.12	18.14	0.38	30.03	0.48	2.52	0.06	0.29
WF1–11.2	13.90	0.11	0.30	22.40	0.04	0.12	17.41	0.38	29.21	0.48	2.22	0.14	0.31
WF1–16.1	10.80	0.11	0.30	25.22	0.04	0.12	13.81	0.38	31.09	0.47	−2.36	0.11	0.30
WF1–16.2	10.97	0.11	0.30	25.95	0.05	0.12	13.97	0.38	31.82	0.47	−2.57	0.13	0.31
WF1–18.1	1.88	0.13	0.30	9.75	0.04	0.12	2.68	0.32	11.29	0.23	−3.20	0.12	0.31
WF1–18.2	1.61	0.12	0.30	8.68	0.04	0.12	2.41	0.32	10.22	0.23	−2.91	0.11	0.30
WF2A-2.1	3.83	0.09	0.29	14.55	0.05	0.12	6.54	0.33	19.82	0.34	−3.76	0.07	0.29
WF2A-2.2	4.37	0.10	0.29	15.68	0.04	0.12	7.08	0.33	20.96	0.33	−3.82	0.11	0.30
WF2A-8.1	1.26	0.10	0.29	15.23	0.05	0.12	2.68	0.33	17.98	0.30	−6.68	0.15	0.32
WF2A-8.2	1.71	0.10	0.29	15.79	0.05	0.12	3.12	0.33	18.54	0.30	−6.52	0.12	0.31
WF2A-20.1	7.03	0.11	0.30	12.36	0.04	0.12	9.59	0.35	17.33	0.37	0.58	0.11	0.30
WF2A-20.2	7.61	0.11	0.30	12.51	0.05	0.12	10.18	0.35	17.48	0.37	1.09	0.10	0.30

Abbreviation: SHRIMP-SI, sensitive high-mass resolution ion micro probe-stable isotope.

studies have isolated a smaller range of $\delta^{18}O$ values for most batches of this material that are acceptable for modern high-precision oxygen isotope applications[32–34] and certainly for use as a SIMS reference material. The use of San Carlos olivine for standardising SIMS measurements of $\delta^{18}O$ was recently reviewed,[11] and we adopt their preferred value for this material of $\delta^{18}O = 5.27‰$ for IMF corrections.

We firstly correct raw oxygen isotope ratios of micrometeorites for IMF using San Carlos olivine, yielding $\delta^{18}O$ and $\delta^{17}O$ in the conventional manner.[1,14] We will refer to values calculated in this way with respect to the San Carlos olivine standard as $\delta^{18}O_{SC}$ and $\delta^{17}O_{SC}$. The repeatability of San Carlos olivine is propagated to internal errors on $\delta^{18}O_{SC}$, $\delta^{17}O_{SC}$ and $\Delta^{17}O_{SC}$ for unknown measurements to obtain 'external' errors (Table 2). An additional correction for phase-related matrix effects will then be made, that is, adjustments for variable glass and magnetite proportions, which will be described in Sections 2.3 and 4. To evaluate matrix effects for glasses by SHRIMP-SI, we analysed the oxygen isotopic compositions of established basaltic glass reference materials BCR-2G, BIR-1G and BHVO-2G, which are commonly used for this purpose.[35–37] We also analysed an in-house iron oxide standard (haematite psuedomorph after magnetite) from the Otago Schist, New Zealand.[38,39] This material has been used as a reference material in LF-IRMS work[40] and will be used to address the matrix effect associated with Fe-oxide, taking it as a proxy for magnetite as found in cosmic spherules. The bulk redox state of Fe in cosmic spherules is probably similar to that of stoichiometric magnetite due to their being mixtures of olivine (containing FeO), magnetite (Fe_3O_4) and glass formed under relatively high partial pressures of O_2 and quite high temperature (mostly Fe_2O_3).

2.3 | Laser-ablation inductively coupled plasma mass spectrometry and outline of matrix effect corrections

After analysis by SIMS, the various cosmic spherules were characterised for their chemical compositions using LA-ICP-MS at Ghent University, Belgium. The concentrations of major and minor elements were determined using a 193 nm ArF* excimer-based Analyte G2 laser ablation system (Teledyne CETAC Technologies, Omaha, USA) coupled to an Element XR (Thermo Fisher Scientific, Bremen, Germany) sector-field ICP-MS unit. Analysis was performed

via single or repeated laser drilling using a laser spot size of 50 μm in diameter, a laser dwell time of 20 s, a repetition rate of 20 Hz and a beam energy density of 2.06 J/cm^2 on the spherule surface, after a round of pre-ablation. The spherules and reference materials were mounted in a standard HELEX 2 double-volume ablation cell. The He carrier gas (0.5 L/min) was mixed with Ar make-up gas downstream of the ablation cell and introduced into the ICP-MS unit, operated at low mass resolution. Precise and accurate element concentration data were obtained based on external calibration, using matrix-matched MPI-DING glasses ATHO-G, GOR 128-G, GOR 132-G, KL2-G, ML3B-G, StHS6/80-G, and T1-G as well as USGS glasses BCR-2G, GSD-1G, and GSE-1G and total oxide normalisation to 100 wt.%. Following this procedure, precise and accurate major and minor element concentrations were obtained for USGS glass BHVO-2G (supporting information Table S1). Based on the analyses of the reference materials, the repeatability for the elements measured is typically on the order of 10% relative standard deviation, depending on the concentration.

In our study, use of relatively broad-beam SIMS and LA-ICP-MS measurements resulted in representative sampling volumes that contain mixtures of predominantly olivine, glass and magnetite. We took the LA-ICP-MS compositions for each sample as approximations of the bulk spherule chemical compositions and recalculated them using a simple least square method into idealised three-component mixtures reflecting the modal mineralogy and bulk compositions. The three idealised end-member components that we have selected are as follows: (1) forsteritic olivine with a Fo_{100} composition; (2) a simplified ferrobasaltic component with 50 mol% SiO_2, 25 mol% FeO, 20 mol% MgO and 5 mol% of other oxides; and (3) a pure Fe-oxide component representing magnetite (80% FeO on a molar basis, or 90% on a weight basis). These three components were used to calculate a unique matrix effect for each spherule and to correct the corresponding oxygen isotope analysis by treating the effect as a linear, weighted average mixture of the individual behaviours for each phase. A small additional inert component was also included in the least square calculation to uniquely describe the bulk composition of each spherule, mainly accounting for excess alumina or other oxides (e.g., spherule WF1–16) but has no influence on determining the matrix effect. Errors were calculated in the same manner, that is, as the weighted average of the analytical uncertainties for each of the three active components. The historical use of these three phases as reference materials in SIMS and the rationale behind our selection of these components will be discussed in detail in Section 4. The method is similar to previous least square approaches to IMF and matrix effects[41–43] and is a considerable improvement over correction assuming a single IMF or universal matrix effect.

3 | RESULTS

The spherule population in our study comprises barred olivine and cryptocrystalline spherules following established textural classification[19] with average particle sizes ranging from 161–203 μm.

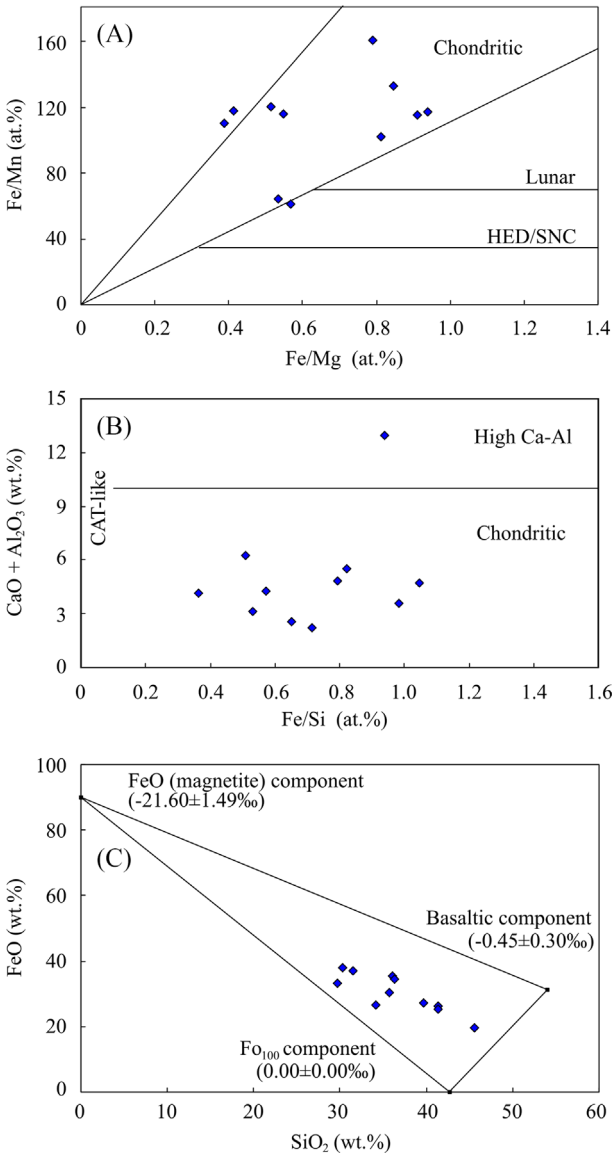

FIGURE 2 Major element compositions of micrometeorites determined by laser ablation inductively coupled plasma mass spectrometry (LA-ICP-MS). All micrometeorites in this study are classified as cryptocrystalline or barred olivine textural types. (A) Fe/Mg versus Fe/Mn diagram (atom ratios) modified from previous classification schemes.[44,45] (B) Fe/Si (atom ratio) versus CaO + Al_2O_3 (weight %) diagram modified from established classification.[46] (C) SiO_2 and FeO contents (weight %) of micrometeorites, along with idealised end-member components for our matrix effect correction (Fo_{100}, basaltic, and Fe-oxide components) and the assigned $\delta^{18}O$ biases for each material [Color figure can be viewed at wileyonlinelibrary.com]

Because of larger chemical variations in other types of spherules (e.g., Ca-Al-Ti 'CAT', metal-oxide 'I-type', or unmelted micrometeorites), we do not address SIMS matrix effects for such micrometeorites in this study. The LA-ICP-MS major and minor oxide compositions of cosmic spherules are given in Table 1 and illustrated in Figure 2. Based on the Fe/Mg versus Fe/Mn diagram, all spherules are essentially chondritic for these ratios (Figure 2A) and unrelated to

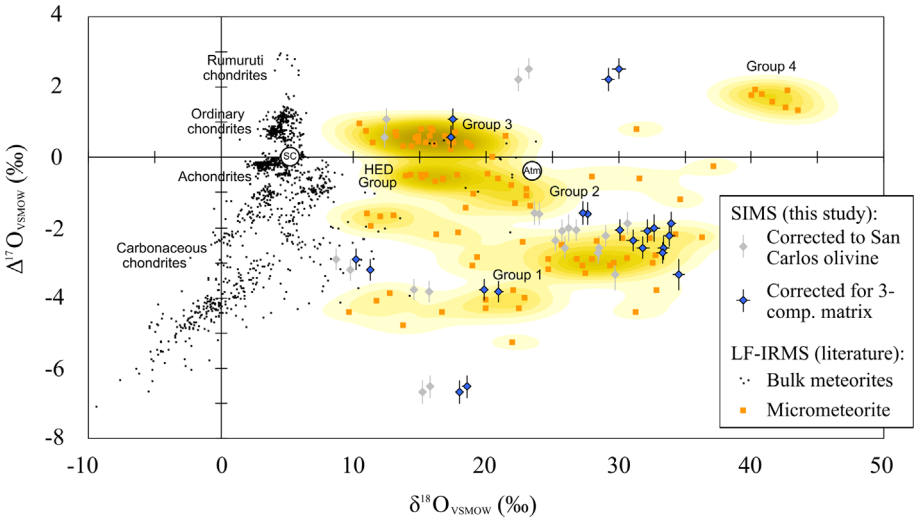

FIGURE 3 Triple oxygen isotope compositions relative to Vienna Standard Mean Ocean Water (VSMOW) for cosmic spherules by secondary ion mass spectrometry (SIMS) using sensitive high-mass resolution ion micro probe-stable isotope (SHRIMP-SI) (this study), small- to mid-sized stony micrometeorites by laser fluorination-assisted isotope ratio mass spectrometry (LF-IRMS)[2,4,16,46,47] and bulk meteorites by LF-IRMS.[48,49] The SIMS values for $\delta^{18}O$ are calculated using an assigned value for San Carlos olivine (SC) of $\delta^{18}O = 5.27‰$.[11] SIMS data are firstly corrected for instrumental mass fractionation (IMF) effects using San Carlos olivine ($\delta^{18}O_{SC}$); these data are given in grey diamonds. Data are secondarily corrected for phase-related matrix effects using our three component mixing model (Fo_{100}, basaltic and Fe-oxide components yielding $\delta^{18}O_{3\text{-comp.}}$); these data are given in blue diamonds. $\Delta^{17}O$ is calculated using a reference line with slope $\lambda = 0.52$. The values for terrestrial atmospheric O_2 (Atm) are $\delta^{18}O = 23.5‰$ and $\Delta^{17}O = -0.4‰$.[50] The SIMS data are presented with 1σ error bars; for clarity, the much smaller analytical errors for LF-IRMS data are omitted. The probability density distribution of small- to mid-sized stony micrometeorite LF-IRMS data is given in yellow fields; these data were contoured using assigned 'geological' or intraspherule 1σ errors of 2.0‰ and 0.2‰ for $\delta^{18}O$ and $\Delta^{17}O$, respectively (see supporting information Table S4) [Color figure can be viewed at wileyonlinelibrary.com]

differentiated achondrites such as the howardite-eucrite-diogenite group; the same is also indicated by the Fe/Si versus $CaO + Al_2O_3$ diagram[44,47] (Figure 2B), where all except one plot in the 'normal chondritic' field; one barred olivine spherule lies in the 'High Ca-Al' field (WF1–16) due to its high Al_2O_3 content. The silica contents of our cosmic spherules are mostly quite low at 29.7–41.4 wt. % SiO_2, except for one basaltic composition (45.5 wt. %; WF1–18). Together they define a trend ranging from a generally basaltic or komatiitic composition towards a 'ferrokomatiitic' composition with lower silica and higher Fe-oxide contents (Figure 2C).

The repeatability of our $\delta^{18}O$ and $\Delta^{17}O$ SIMS measurements was primarily assessed through the behaviour of San Carlos olivine, for which we achieved standard deviations of 0.11‰ and 0.28‰, respectively ($n = 47$, 1 reject; supporting information Table S2). Secondary beam current yields are slightly higher in cosmic spherules than in San Carlos olivine (Table S3 and Figure S1), but among cosmic spherules, yields are only weakly related to major element compositions or assigned phase components (Figure S2). This suggests that grain-scale interconnectivity and local conduction effects may be more important controls on total ion yield. Most of our cosmic spherules have negative $\Delta^{17}O$, and all have strongly positive $\delta^{18}O_{SC}$. Our data, as for most collections, cover a wide range of oxygen isotope compositions with $\delta^{18}O_{SC}$ and $\Delta^{17}O$ (average of each replicate) ranging from +8.7‰ to +30.7‰ and −6.7 to +2.5‰, respectively (Table 2 and grey symbols in Figure 3). Regarding intraspherule variations, for each duplicate pair, $\delta^{18}O$ are within 1.25‰ of each other with one exception at 3.9‰ and $\Delta^{17}O$ within 0.6‰ in all cases.

For our in-house iron oxide standard, over two analytical sessions, we found strong IMF effects for SHRIMP-SI that biassed $\delta^{18}O$ to strongly negative compositions compared to silicates. We found average $\delta^{18}O_{SC}$ for iron oxide of −24.52‰ (standard deviation 0.53‰; $n = 5$) and −21.54‰ (standard deviation 0.43‰; $n = 5$) for each analytical session, which are much lower than the composition from LF-IRMS (−1.43‰).[40]

While the aim of our study is to assess phase-related matrix effects superimposed upon $\delta^{18}O_{SC}$, the $\Delta^{17}O$ obtained by SIMS is already a good indicator of the possible nebular or planetary source, that is, the major micrometeorite Groups 1 to 4.[2] In order to facilitate comparison, we use the previously published LF-IRMS data for stony micrometeorites to provide an up-to-date definition of the micrometeorite groups. While the reported analytical errors for LF-IRMS studies are very precise, the effective 'geological' or intraspherule error that arises from melting in the atmosphere is somewhat larger (e.g., several per mille).[14] Therefore, we generated a probability density contour plot from previous LF-IRMS studies of small and mid-sized stony micrometeorite compositions. In this contouring, we assume 1σ errors for $\delta^{18}O$ and $\Delta^{17}O$ of 2.0‰ and 0.2‰, respectively (source data given in supporting information Table S4).[2,4,16,46,47] We exclude ~1 mm or larger 'giant' cosmic spherules that are mostly in Group 3,[51] and iron-rich I-types that do not contain significant silicates. Overlay of our SIMS $\delta^{18}O_{SC}$ and

$\Delta^{17}O$ in Figure 3 onto the probability density contours suggests that of our 11 samples, seven are associated with Groups 1 and 2 (mainly carbonaceous chondrite-related). Sample WF2A-20 falls in the field of Group 3 (ordinary chondrite-related), and sample WF1-11 is at higher $\Delta^{17}O$ similar to Group 4 but with much lower $\delta^{18}O_{SC}$. Two samples (WF1-18 and WF2A-8) are dissimilar to the main micrometeorite groups because of lower $\delta^{18}O_{SC}$ or $\Delta^{17}O$ suggestive of a substantial relict content. In the next section, we will make an additional correction to $\delta^{18}O_{SC}$ that will account for interphase matrix effects between olivine, basaltic glass and Fe-oxide, using the major oxide compositions of each spherule (giving $\delta^{18}O_{3\text{-comp.}}$ and $\delta^{17}O_{3\text{-comp.}}$). This will be discussed in Section 4.4 after reviewing SIMS matrix effects related to olivine, basaltic glass and other oxide components.

4 | DISCUSSION

4.1 | Olivine

Most studies of the triple oxygen isotopic compositions of cosmic spherules, including ours, utilise San Carlos olivine as a primary standard to correct IMF. While this method is particularly applicable to measurements of olivine with a composition close to Fo_{90}, such olivine is not the only phase and need not be present at all in cosmic spherules. Natural olivine compositions often vary widely and can be zoned within single crystals. In addition to olivine, finely crystalline stony cosmic spherules contain glass and magnetite almost without exception. Here and in the following sections, we review previous SIMS triple-oxygen isotope studies of olivine, glass and magnetite and assess how variable proportions of these phases or heterogeneity in their compositions might drive stronger or weaker analytical artefacts or biases. Such phase-specific processes, that is, 'matrix effects', are likely to influence obtained ion ratios during analysis of cosmic spherules. It should be noted that the terms IMF and matrix effect have been used interchangeably in the literature. For our specific methodological development using SHRIMP-SI, we will refer to the use of San Carlos olivine to monitor instrumental behaviour as an 'IMF correction' (discussed in the previous sections and yielding $\delta^{18}O_{SC}$). The difference in fractionation behaviour between phases such as basaltic glass and Fe-oxide, and especially relative to San Carlos olivine, will be referred to as a matrix effect.

There are numerous studies that have investigated matrix effects for oxygen isotopes in olivine by SIMS. In large probes (e.g., CAMECA 1270 onwards and SHRIMP), high-mass resolution is used to separate molecular interferences such as $^{16}O^{1}H^{+}$.[13,21,52] Ion probe IMF effects on triple oxygen isotopes in olivine are a function of $Fo_{\#}$.[10,53] With CAMECA probes, most studies indicate that IMF is constant between Fo_{80-100}, but ratios become strongly biassed towards lower values with increasing FeO content, until reaching values of approximately 9‰ lower than San Carlos olivine at the pure fayalite end-member.[10,54]

The behaviour of SHRIMP ion probes has been found to be similar to CAMECA probes but in detail there are some differences in the $Fo_{\#}$-IMF relationship. An investigation of this behaviour using SHRIMP-II and SHRIMP-SI[11] found uncorrected $^{18}O^{-}/^{16}O^{-}$ for magnesian olivine to be biassed towards values 5.5‰–8‰ higher than LF-IRMS values, as a function of $Fo_{\#}$ in the range Fo_{74} to Fo_{100} (their S1 and S2). The maximum positive IMF bias lies at around Fo_{81} and decreases again by ~1.5‰ on close approach to Fo_{100} (their Figure 2).[11] Although continuous variation in IMF with $Fo_{\#}$ can be inferred for well characterised olivine samples, including the maximum bias at Fo_{81}, the effect is close to resolution. In fact, most of the magnesian olivine in that study exhibited bias at similar levels to that of San Carlos olivine, and the matrix effect became detectable only for FeO-rich olivine and for nearly pure forsterite.[11] Considering the nearly stable SHRIMP matrix effect within the compositional range of Fo_{74-91} and similar general trends for CAMECA probes, it is reasonable to approximate this behaviour for a required precision. This is in fact the standard approach to IMF employed by many studies that use San Carlos olivine as their primary reference material. We will make no specific correction for olivine (whether as a discrete phase or cryptic component), and in our corrections going forward, we will use an idealised Fo_{100} component as the starting point for modelling matrix effects, that is, building upon $\delta^{18}O_{SC}$ defined previously.

4.2 | Basaltic glass

With the availability of large radius ion probes, moderate and reproducible degrees of IMF were achieved in the range of several per mille, enabling matrix effects in glasses to be addressed. This has been much applied to basaltic glass and glass inclusions in phenocryst-bearing lavas, and especially by CAMECA probes. For example, early work using a wide range of glass reference materials over several analytical sessions found oxygen isotope IMF to be negatively correlated with SiO_2 and less strongly positively correlated with FeO and CaO.[12] In that study, a relationship for IMF of 0.05–0.38 per mille per wt. % SiO_2 was found to be sufficient to correct analyses to within achieved analytical precision.[12] In subsequent work in the same lab, the same relationship was found, but the use of a single IMF value for basaltic materials to be appropriate because slope was effectively controlled by a single reference glass at higher SiO_2.[55] In a follow-up study, also in the same lab, a similar SiO_2 control on IMF was found across multiple phases including glassy mesostatis in chondrules, with IMF minimising and stabilising at SiO_2 contents less than ~45 wt.%.[56] Other SIMS labs also found IMF to be strongly controlled by SiO_2 and less so by CaO and FeO, with satisfactory corrections being possible using SiO_2 alone, although the strength and details of the relationship vary between instruments.[35–37] While variation can of course be generated by manipulating instrumental settings, the general trends in IMF with SiO_2 in glass and $Fo_{\#}$ in olivine are fairly robust.

For SHRIMP-II, previous work on the oxygen isotope IMF for basaltic and other glassy materials found that uncorrected $^{18}O^{-}/^{16}O^{-}$ values are, like olivine, variably biassed to positive values and increase

with decreasing SiO_2 towards a plateau at basaltic compositions (45–52 wt.% SiO_2).[13] We re-investigated IMF effects in glasses using SHRIMP-SI to obtain a calibration specific to our measurements. Basaltic to basaltic andesitic glasses BCR-2G, BHVO-2G and BIR-1G were analysed alongside San Carlos olivine under the same conditions as our micrometeorite measurements. From comparison with accepted LF-IRMS values,[57,58] for the lower silica glasses BHVO-2G and BIR-1G, we found $\delta^{18}O$ to be only very slightly biassed towards lower values (near limits of resolution, at −0.03 ± 0.09‰ and −0.06 ± 0.07‰ (1 std. dev., $n = 5$ for both glasses), but for the higher silica glass BCR-2G, we found a stronger bias of −1.54 ± 0.15‰ (1 std. dev., $n = 5$). To currently achieved precision, and as found by other studies for both CAMECA and SHRIMP probes, the oxygen isotope IMF correction for glasses by SHRIMP-SI is mainly controlled by SiO_2 and rather insensitive to the contents of other oxides in the matrix.

Building upon our use of San Carlos olivine to obtain $\delta^{18}O_{SC}$ for micrometeorites, we will assign a basaltic glass component to account for matrix effects. Because of the microcrystalline nature of most cosmic spherules and the associated difficulty with obtaining precise major element compositions for any interstitial glass, even by modern EMPA methods, we will not attempt a detailed IMF correction method for this phase. Rather, we apply an idealised ferrobasaltic composition of 50 mol% SiO_2, 25 mol% FeO, 20 mol% MgO, and 5 mol% of other oxides. For the three basaltic glass reference materials we have analysed, an inverse-error weighted linear regression of SiO_2 against observed bias yields an SiO_2-corrected bias of −0.45 ± 0.30‰ (1-sigma) for our idealised ferrobasaltic component with respect to San Carlos olivine that we will use to determine $\delta^{18}O_{3\text{-comp.}}$ for our unkowns (Table 3). One may question whether the relationship is strictly linear and this is worth investigating in the future, but the effect is anyway small for glasses with basaltic silica levels. The idealised ferrobasaltic composition that we have selected represents a compromise between what is known about oxygen isotope IMF for silicate glasses investigated so far by SIMS (basaltic to rhyolitic and various synthetic glasses) and achieving coverage of the micrometeorite compositions in our study (generally basaltic to ferrokomatiitic).

TABLE 3 End-member three-component matrix effects relative to San Carlos olivine for correction of $\delta^{18}O_{SC}$ for micrometeorites obtained by sensitive high-mass resolution ion micro probe-stable isotope (SHRIMP-SI); all values in per mille (‰). The Fo_{100} value is set to zero reflecting use of San Carlos olivine as the primary reference material. The basaltic value is obtained by an inverse-error weighted regression of the three basaltic glasses corrected to 50 wt.% SiO_2. The value for magnetite is the average of the Otago schist iron oxide in-house standard (haematite pseudomorph after magnetite) over two analytical sessions

Component	Fo_{100}[a]	Basalt	Magnetite
Matrix effect	0.00	−0.45	−21.60
Std. err.	0.00	0.30	1.49

[a]In our method, the Fo_{100} component requires no correction for matrix effect, that is, we assume that it corresponds to San Carlos olivine, which is used as the primary reference material with an assigned $\delta^{18}O$ composition of 5.27‰[11] and using our repeatability propagated to external errors of unknowns.

4.3 | Fe-oxide and remaining oxides

In early work on magnetite using a small ion probe, large negative IMF values were observed,[59] similar to that found for equivalent nonconductive phases, and an orientation effect was inferred from poor grain-to-grain repeatability. This orientation effect was confirmed by further studies using similar ion probes[60,61] and eventually by larger CAMECA ion probe in which a 2‰–3‰ effect was found.[62] Such effects are driven by channelling of primary ions and focussing of secondary ions during analysis of crystals with high-symmetry such as magnetite, with a similar effect in haematite as well.[62]

The SHRIMP model ion probes have not previously been used to investigate IMF or orientation effects in iron oxides. We used SHRIMP-SI to analyse an in-house iron oxide standard (haematite pseudomorph after magnetite) from the Otago Schist, New Zealand ($\delta^{18}O = -1.43$‰),[40] again under the same conditions as given in the previous sections. Because we anticipated an orientation effect, we analysed two different pieces (one in each of two analytical sessions) finding behaviour differing outside of analytical error. Both were strongly biassed towards negative $\delta^{18}O_{SC}$ with values of −24.52 ± 0.53‰ and −21.54 ± 0.43‰ (1 standard deviation; $n = 5$ in both sessions). The relatively large variation indicates that SHRIMP is, as expected, affected by orientation effects found by grain-to-grain comparisons of magnetite and haematite with CAMECA ion probes.[59,62]

We take the average $\delta^{18}O_{SC}$ for the iron oxide from the Otago Schist, New Zealand, to determine a matrix effect for the pure Fe-oxide component of −21.60 ± 1.49‰ (1-sigma) that we use to determine $\delta^{18}O_{3\text{-comp.}}$ for our unkowns (Table 3). It is unlikely that orientation effects would be analytically significant for stony cosmic spherules because they typically contain many tiny magnetite crystals that are much smaller than the scale of sampling, and our intention here is to build up a long-term average for our Fe-oxide reference material over several analytical sessions in this and future work. While the pure Fe-oxide component naturally represents magnetite occurring as discrete crystals in micrometeorites, it is worth noting that the sense of change found for admixture of magnetite is the same as for increasing amounts of FeO-rich olivine. This may be roughly consistent with a linear mixture of an additional fayalitic olivine end-member depending on assumed IMF values for the Fe-oxide component and the particular relationship with $Fo_{\#}$. Such an effect might be worth considering in future studies of particularly fayalite-rich micrometeorites.

To complete the bulk rock composition, we also define an inert component representing all remaining oxides, which we refer to as 'other oxides' (Table 1). In our method, this component plays no part in the correction and is only used to fully account for the major and

minor oxide composition. This closes the modelled major element compositions to 100% and achieves a least square solution to the bulk composition. Its main effect is to accommodate alkalis or excess alumina and is less than 5.1% in all spherules except for WF1-16, in which it is 14.7% (due to high Al_2O_3) but is not used in determining the matrix effect.

4.4 | Application of three-component matrix effect correction and comparison of SIMS data with major stony micrometeorite groups

While some triple oxygen isotope data for grouped stony and iron cosmic spherules were reported in early work,[63] the outlining of major isotopic micrometeorite groups was not made until analysis of single micrometeorites by LF-IRMS became possible. Most of these samples were recovered from the Transantarctic Mountains. The first such measurements were presented as a dataset from two laboratories for 33 melted silicate micrometeorites.[2] These data defined four major micrometeorite groups: Group 1 having the lowest $\Delta^{17}O$ (related to CO/CV carbonaceous chondrites), Group 2 with moderately negative $\Delta^{17}O$ (related to CM/CR carbonaceous chondrites and possibly achondrites), Group 3 with slightly positive $\Delta^{17}O$ (related to ordinary chondrites) and Group 4 with the highest $\Delta^{17}O$ and $\delta^{18}O$ (possibly related to Rumuruti chondrites or another reservoir). A further 25 such LF-IRMS measurements[46,51] confirmed a suspected increase in ordinary chondrite parentage as the size of cosmic spherules increases (most obviously for 'giant' micrometeorites reported in the latter). Some stony micrometeorites with an achondritic source, specifically with Howardite-Eucrite-Diogenite (HED) affinities, can be distinguished from Group 2 micrometeorites through dedicated petrographic and geochemical study.[47] The global occurrence of the major groups in suitable sedimentary traps has since been confirmed by 18 spherules from the Atacama Desert in South America[16] and 28 from the Sør Rondane Mountains in East Antarctica.[4] Our contouring of the probability density distribution of LF-IRMS data provides a starting point to assess the distributions of these groups in triple oxygen isotope space (Figure 3). While the locations and shapes of each group are informative, it should be kept in mind that the larger micrometeorites suitable for LF-IRMS are preferentially affiliated with Group 3, so the peak heights for each group are not directly comparable with the distributions obtained from smaller micrometeorites. The transition from majority carbonaceous to ordinary chondrite sources occurs at micrometeorite diameters of ~500 μm.[3]

With each of our replicate 'intraspherule' $\delta^{18}O_{SC}$ measurements being within 1.2‰ of each other with one exception at 3.9‰ and $\Delta^{17}O$ within 0.6‰ in all cases, our analyses can resolve microscale variations in the amount of terrestrial atmospheric oxygen taken up by a spherule during entry and melting. These data compare favourably with previous measurements that found ~5‰ intraspherule variation for $\delta^{18}O$ in most spherules.[14] For major and minor elements, most spherule compositions obtained by LA-ICP-MS are well accommodated by our three-component mixing model (10 from 11 spherules; Figure 2C and Table 1) except for WF2A-2, which requires a negative basaltic component (−15.6%) due to its high MgO content. The most aluminous spherule WF1–16 relies strongly on the inert 'other oxides' component (14.7%), which in other spherules is quite low (up to 5.1%) (Table 1). There is a slight preference for BO and BO/Cc type spherules to have compositions nearer the Fo_{100}-FeO tie-line, while Cc-type spherules are nearer our assumed ferrobasaltic component, although there is overlap among all types. The required correction for matrix effects is mostly analytically significant, that is, larger than statistical errors arising through analysis by SHRIMP-SI using San Carlos olivine as the primary standard. We take the three components from our mixing model as the weightings to calculate the matrix effect; that is, we assume the mixing is linear, although other weightings are certainly possible based on other criteria. In quantifying the precision of our measurements, we take the internal and external errors for $\delta^{18}O_{SC}$ and $\delta^{17}O_{SC}$ (Table 2) propagated with uncertainties on the matrix effect (Table 3) to obtain 'standard errors' for $\delta^{18}O_{3\text{-comp.}}$ and $\delta^{17}O_{3\text{-comp.}}$ values (Table 2). Overall, the strength of the matrix effect is similar to or slightly greater than the intraspherule repeatability. Required corrections to $\delta^{18}O_{SC}$ yielding $\delta^{18}O_{3\text{-comp.}}$ are in the range −1.5 ± 0.2‰ to −6.6 ± 0.5‰ (Table 1) and are naturally largest for spherules with compositions that are far from idealised Fo_{100} and closer to Fe-oxide (Table 3). A comparison between $\delta^{18}O_{SC}$ and $\delta^{18}O_{3\text{-comp.}}$ is given in Figure 3, where these data are plotted against $\Delta^{17}O$, which is unmodified by corrections for IMF and matrix effects because instrumental effects are mass-dependent, that is, horizontal translations in a $\delta^{18}O$-$\Delta^{17}O$ plot.

The majority of our analyses fall in the major Group 1 micrometeorite field with $\Delta^{17}O$ below −2‰, while others are more widely scattered in triple oxygen isotope space (Figure 3). The $\delta^{18}O_{SC}$ of our Group 1 analyses fall mostly near the middle of that group, but their corrected $\delta^{18}O_{3\text{-comp.}}$ lie near the higher end, in the range of $\delta^{18}O$ from approximately +30‰ to +35‰. Other samples are more widely distributed across the major groups or lie outside them. At slightly lower $\Delta^{17}O$, sample WF2A-2 also lies within the broader Group 1. At slightly higher $\Delta^{17}O$, WF1-1 lies near the margin of Group 2. At slightly positive $\Delta^{17}O$, WF2A-20 lies in the Group 3 field with $\delta^{18}O_{3\text{-comp.}}$ having been brought very close to the centre of this group by the correction. At yet higher $\Delta^{17}O$, WF1-11 lies in a thinly populated region of triple-oxygen isotope space and has been brought closer to the Group 4 micrometeorites by the three-component correction. Despite having the largest correction, it still lies outside the main Group 4 distribution with which it is probably associated. Finally, two samples at lower $\Delta^{17}O$ and $\delta^{18}O$, respectively, are outside the major micrometeorite groups, suggestive of substantial relict content and only moderate processing in the atmosphere.

The original definition of four major stony micrometeorite groups[2] has been shown through further work to be broadly correct for larger micrometeorites.[4,16,46] Groups 3 and 4 are especially clear, as shown by their well resolved probability density peaks in Figure 3. These two groups may be most obvious because of a coherent

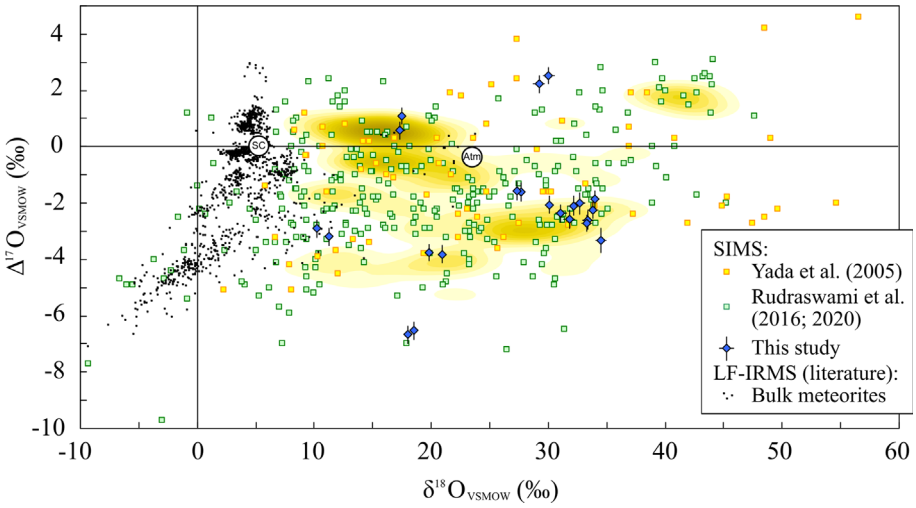

FIGURE 4 Triple oxygen isotope compositions relative to Vienna Standard Mean Ocean Water (VSMOW) for stony cosmic spherules by secondary ion mass spectrometry ((SIMS) from the literature[5,7,9] (excluding relict, chromite-bearing and I-type spherules) and this study (sensitive high-mass resolution ion micro probe-stable isotope [SHRIMP-SI]). Bulk meteorite data by LF-IRMS[48,49] and contoured probability density distribution of small- to mid-sized stony micrometeorites by LF-IRMS[2,4,16,46,47] (as for Figure 3, with assigned 1σ errors of 2.0‰ and 0.2‰ for $\delta^{18}O$ and $\Delta^{17}O$, respectively; see supporting information Table S4). $\Delta^{17}O$ is calculated using a reference line with slope $\lambda = 0.52$. Values for terrestrial atmospheric O_2 (Atm) are $\delta^{18}O = 23.5‰$ and $\Delta^{17}O = -0.4‰$.[50] Data from SHRIMP-SI are given in blue diamonds; our values of $\delta^{18}O$ are calculated using an assigned value for San Carlos olivine (SC) of $\delta^{18}O = 5.27‰$[11] and are corrected for phase-related matrix effects using our three component mixing model (Fo_{100}, basaltic, and Fe-oxide components yielding $\delta^{18}O_{3\text{-comp.}}$). Analytical errors for SHRIMP-SI data are presented with 1σ error bars; for clarity, we omit the error bars for all other SIMS data. A few SIMS data from other studies at extreme $\delta^{18}O$ and $\Delta^{17}O$ are not shown at this scale [Color figure can be viewed at wileyonlinelibrary.com]

ordinary chondrite source for Group 3, their positions above the terrestrial fractionation line at positive $\Delta^{17}O$ and the difficulty in materials crossing this line during atmospheric processing. The probability density distributions generated by our contouring method for Groups 1 and 2 (latter including the HED-group) are considerably more complex. Our contouring suggests that subsets of Groups 1 and 2 contain a higher relict content (at lower $\delta^{18}O$) and may be distinct according to the probability distribution. One of our own points lies in the extended Group 1, and the large number of data presented by previous studies[5,7,9] suggests that this cryptic relict material is regularly sampled but unrecognised. Nevertheless, it is not clear whether this complexity is significant and whether it arises from some preferential sources among the carbonaceous chondrites combined with atmospheric processing under typical entry angles and velocities.[64,65]

While modern LF-IRMS data seem to justify the major micrometeorite groups, the previously published SIMS data, on the other hand, show a more continuous distribution across triple oxygen isotope space when the largest datasets are considered (Figure 4). While this might be expected from a larger number of less precise analyses, the distributions reported among recent SIMS data also show variations from one study to another. These variations are likely related to preferential selection of certain types of micrometeorites, mineral targets and possibly analytical biases in each study, for example, multiphase sampling or unrecognised matrix effects.

Some SIMS studies focussed on relict materials and need not be directly compared with the major stony micrometeorite groups or considered when addressing high degrees of atmospheric processing.[1,6,66] Other studies included fewer data relating to relict grains and mainly reported processed materials similar to those we have studied, that is, cosmic spherules. Early studies of Antarctic micrometeorites made substantial progress in understanding isotopic processing of micrometeorites during atmospheric entry.[5,14,15] However, of these early SIMS studies, only one[5] presented data for enough samples to achieve good coverage of the triple oxygen isotope space, with 48 cosmic spherules widely distributed across all four major stony micrometeorite groups and also in previously thinly populated regions of triple oxygen isotope space.

Subsequently, additional SIMS datasets for the triple oxygen isotopes of small micrometeorites were published.[7–9] One of these[8] focussed on a set of chromite-bearing stony micrometeorites ($n = 18$), finding most to be related to ordinary chondrites, which are a known source of extraterrestrial chromite delivery to the Earth.[67] Larger datasets of stony cosmic spherules from the Indian Ocean and Antarctica[7,9] ($n = 57$ and $n = 122$, respectively) comprised analyses of olivine and magnetite (I-type spherules were also presented in the latter study). These studies reported very wide ranges in oxygen isotope compositions and a large number of Group 1 and 2 spherules with negative $\Delta^{17}O$, consistent with expectations that carbonaceous chondrites are the main sources for such small micrometeorites. Unlike for the LF-IRMS data used to define the major stony micrometeorite groups, the distinctions between the Groups 1 and 2 are not obvious from the large SIMS datasets,[5,7,9] and only the very largest dataset contained a substantial number of

Group 4 micrometeorites at high $\Delta^{17}O$ and $\delta^{18}O$.[9] In that study, a potential correlation was found between petrographic type and $\delta^{18}O$. This was not found previously.[5] It is likely that all these studies reported oxygen isotope analyses made via SIMS multiphase sampling but with no particular attention to instrumental or matrix effects aside from those for olivine and perhaps magnetite separately.

The particle size range for samples in our study is similar to that of the largest datasets[5,7,9] with nearly all spherule diameters less than ~300 μm. Our dataset of 11 Antarctic micrometeorites by SHRIMP-SI utilises recent improvements in understanding of IMF processes for this type of instrument and in SIMS generally, addressing phase-related matrix effects for basaltic glass, olivine and Fe-oxides determined in this study and previously.[10,11,13,21,52] While the number of samples we have reported is so far small and below the minimum for proper representative sampling, we have found spherules across Groups 1 to 3 and a few outside these groups, one of which at high $\Delta^{17}O$ may have a relationship with Group 4 or Rumuruti chondrites. The clustering of many of our spherules in the region of Group 1 suggests that matrix effects might be responsible for some of the very large spread of SIMS compositions reported previously. We will expand this dataset in subsequent publications as we refine our method. Our study indicates, for SHRIMP style ion probes and probably others as well, that matrix effects in multiphase SIMS samples are generally several per mille, and the degree of bias is sensitive to the proportions of each phase. Such effects are analytically significant because they are comparable to the distributions of the established micrometeorite groups in triple oxygen isotope space and to intraspherule variations reported in previous SIMS studies.[14] Similar effects for CAMECA ion probes would also be significant at currently reported analytical precisions and is a worthwhile avenue to pursue.

5 | CONCLUSIONS

Frequently in SIMS research, the use of a well characterised or well-known primary reference material is commonplace in order to control IMF processes, but such materials, for example, San Carlos olivine, are not necessarily a good match for the target unknown materials. In the study of triple oxygen isotopes of micrometeorites, and especially stony cosmic spherules which are fine grained crystalline igneous samples, microbeam sampling of a single phase is frequently difficult or impossible, and this may induce poorly understood matrix effects. Therefore, following recent developments in understanding matrix effects for SHRIMP style ion probles, we have developed a generic approach to correcting matrix effects in analysis of finely crystalline cosmic spherules, using the bulk major oxide composition of each cosmic spherule from another technique (LA-ICP-MS) recalculated into three well-understood components: forsteritic olivine (Fo_{100}), an idealised ferrobasaltic glass, and Fe-oxide (magnetite). Matrix effects relative to San Carlos olivine for $\delta^{18}O$ are in the range −1.5 ± 0.2‰ to −6.6 ± 0.5‰ and are largest for those with a higher Fe-oxide component. After correction for this effect, intraspherule precision is now the limiting factor in understanding the $\delta^{18}O$ compositions of cosmic spherules, at ~5‰.[14] Previous SIMS studies have made no specific attempt to correct for these matrix effects[5] or have addressed phases such as olivine and Fe-oxide separately.[9] In the future, triple oxygen isotope datasets of cosmic spherules may benefit from assessment of these effects. Addressing olivine, basaltic glass, Fe-oxide and other relevant components simultaneously may reduce systematic instrumental bias for multiphase samples and enable improved knowledge of bulk-cosmic spherule compositions.

AUTHOR CONTRIBUTIONS

The project was conceived by Seann J. McKibbin, Matthias Van Ginneken, Steven Goderis, Vinciane Debaille and Philippe Claeys; sample collection and initial processing were undertaken by Matthias Van Ginneken, Bastien Soens, Flore Van Maldeghem, Steven Goderis, Vinciane Debaille and Philippe Claeys; samples were characterised by Bastien Soens and Flore Van Maldeghem; SHRIMP analyses were made by Janaína N. Ávila, Leonardo Baeza, Aditya Patkar and Trevor R. Ireland; LA-ICP-MS analyses were made by Bastien Soens, Steven Goderis and Frank Vanhaecke; data from the literature were processed by Matthew Huber; Seann J. McKibbin wrote the first draft of the manuscript, and all authors contributed to the final version of the manuscript.

ACKNOWLEDGEMENTS

We thank Oliver Steenhaut, Peter Holden, Peter Lanc and Stijn Van Malderen for assistance with sample imaging and analysis throughout the course of this project. We also thank Ryan Ickert and an anonymous reviewer for their critical reviews and suggested improvements to the manuscript. This research was supported by postdoctoral fellowships to SMcK from the Research Foundation–Flanders (FWO) and the Alexander von Humboldt Foundation. Additional support was provided by FWO grant 11C2520N to FVM, the Interuniversity Attraction Poles Program (IUAP) Planet Topers and the BRAIN-be BAMM! projects initiated by the Belgian Science Policy Office and the FWO/FNRS Excellence of Science project ET-HoME (ID 30442502). Open access publishing facilitated by Australian National University, as part of the Wiley - Australian National University agreement via the Council of Australian University Librarians.

CONFLICT OF INTEREST STATEMENT

There are no conflicts to declare.

DATA AVAILABILITY STATEMENT

The data that supports the findings of this study are available in the supplementary material of this article.

PEER REVIEW

The peer review history for this article is available at https://www.webofscience.com/api/gateway/wos/peer-review/10.1002/rcm.9921.

ORCID

Frank Vanhaecke https://orcid.org/0000-0002-1884-3853

Philippe Claeys https://orcid.org/0000-0002-4585-7687

Steven Goderis https://orcid.org/0000-0002-6666-7153

REFERENCES

1. Engrand C, McKeegan KD, Leshin L. Oxygen isotopic compositions of individual minerals in Antarctic micrometeorites: further links to carbonaceous chondrites. *Geochim Cosmochim Acta*. 1999;63(17):2623-2636. doi:10.1016/S0016-7037(99)00160-X
2. Suavet C, Alexandre A, Franchi IA, et al. Identification of the parent bodies of micrometeorites with high-precision oxygen isotope ratios. *Earth Planet Sci Lett*. 2010;293(3-4):313-320. doi:10.1016/j.epsl.2010.02.046
3. Cordier C, Folco L. Oxygen isotopes in cosmic spherules and the composition of the near earth interplanetary dust complex. *Geochim Cosmochim Acta*. 2014;146:18-26. doi:10.1016/j.gca.2014.09.038
4. Goderis S, Soens B, Huber MS, et al. Cosmic spherules from Widerøefjellet, Sør Rondane Mountains (East Antarctica). *Geochim Cosmochim Acta*. 2020;270:112-143. doi:10.1016/j.gca.2019.11.016
5. Yada T, Nakamura T, Noguchi T, et al. Oxygen isotopic and chemical compositions of cosmic spherules collected from the Antarctic ice sheet: implications for their precursor material. *Geochim Cosmochim Acta*. 2005;69(24):5789-5804. doi:10.1016/j.gca.2005.08.002
6. Rudraswami NG, Prasad MS, Nagashima K, Jones RH. Oxygen isotopic composition of relict olivine grains in cosmic spherules: links to chondrules from carbonaceous chondrites. *Geochim Cosmochim Acta*. 2015;164:53-70. doi:10.1016/j.gca.2015.05.004
7. Rudraswami NG, Prasad MS, Jones RH, Nagashima K. In situ oxygen isotope compositions in olivines of different types of cosmic spherules: an assessment of relationships to chondritic particles. *Geochim Cosmochim Acta*. 2016;194:1-14. doi:10.1016/j.gca.2016.08.024
8. Rudraswami NG, Marrocchi Y, Shyam Prasad M, Fernandes D, Villeneuve J, Taylor S. Oxygen isotopic and chemical composition of chromites in micrometeorites: evidence of ordinary chondrite precursors. *Meteorit Planet Sci*. 2019;54(6):1347-1361. doi:10.1111/maps.13281
9. Rudraswami NG, Genge MJ, Marrocchi Y, Villeneuve J, Taylor S. The oxygen isotope compositions of large numbers of small cosmic spherules: implications for their sources and the isotopic composition of the upper atmosphere. *J Geophys Res*: Planets, e2020JE006414. 2020;125(10). doi:10.1029/2020JE006414
10. Isa J, Kohl IE, Liu MC, Wasson JT, Young ED, McKeegan KD. Quantification of oxygen isotope SIMS matrix effects in olivine samples: correlation with sputter rate. *Chem Geol*. 2017;458:14-21. doi:10.1016/j.chemgeo.2017.03.020
11. Scicchitano MR, Rubatto D, Hermann J, Majumdar AS, Putnis A. Oxygen isotope analysis of olivine by ion microprobe: matrix effects and applications to a serpentinised dunite. *Chem Geol*. 2018;499:126-137. doi:10.1016/j.chemgeo.2018.09.020
12. Gurenko AA, Chaussidon M, Schmincke H-U. Magma ascent and contamination beneath one intraplate volcano: evidence from S and O isotopes in glass inclusions and their host clinopyroxenes from Miocene basaltic hyaloclastites southwest of gran Canaria (Canary Islands). *Geochim Cosmochim Acta*. 2001;65(23):4359-4374. doi:10.1016/S0016-7037(01)00737-2
13. Ickert RB, Hiess J, Williams IS, et al. Determining high precision, in situ, oxygen isotope ratios with a SHRIMP II: analyses of MPI-DING silicate-glass reference materials and zircon from contrasting granites. *Chem Geol*. 2008;257(1–2):114-128. doi:10.1016/j.chemgeo.2008.08.024
14. Engrand C, McKeegan KD, Leshin LA, et al. Isotopic compositions of oxygen, iron, chromium, and nickel in cosmic spherules: toward a better comprehension of atmospheric entry heating effects. *Geochim Cosmochim Acta*. 2005;69(22):5365-5385. doi:10.1016/j.gca.2005.07.002
15. Taylor S, Alexander CMO, Delaney JS, Ma P, Herzog GF, Engrand C. Isotopic fractionation of iron, potassium, and oxygen in stony cosmic spherules: implications for heating histories and sources. *Geochim Cosmochim Acta*. 2005;69(10):2647-2662. doi:10.1016/j.gca.2004.11.027
16. van Ginneken M, Gattacceca J, Rochette P, et al. The parent body controls on cosmic spherule texture: evidence from the oxygen isotopic compositions of large micrometeorites. *Geochim Cosmochim Acta*. 2017;212:196-210. doi:10.1016/j.gca.2017.05.008
17. Ireland TR, Schram N, Holden P, et al. Charge-mode electrometer measurements of S-isotopic compositions on SHRIMP-SI. *Int J Mass Spectrom*. 2014a;359:26-37. doi:10.1016/j.ijms.2013.12.020
18. Love SG, Brownlee DE. Heating and thermal transformation of micrometeoroids entering the Earth's atmosphere. *Icarus*. 1991;89(1):26-43. doi:10.1016/0019-1035(91)90085-8
19. Genge MJ, Engrand C, Gounelle M, Taylor S. The classification of micrometeorites. *Meteorit Planet Sci*. 2008;43(3):497-515. doi:10.1111/j.1945-5100.2008.tb00668.x
20. van Ginneken M, Genge MJ, Folco L, Harvey RP. The weathering of micrometeorites from the Transantarctic Mountains. *Geochim Cosmochim Acta*. 2016;179:1-31. doi:10.1016/j.gca.2015.11.045
21. Kita NT, Ushikubo T, Fu B, Valley JW. High precision SIMS oxygen isotope analysis and the effect of sample topography. *Chem Geol*. 2009;264(1–4):43-57. doi:10.1016/j.chemgeo.2009.02.012
22. McKinney CR, McCrea JM, Epstein S, Allen HA, Urey HC. Improvements in mass spectrometers for the measurement of small differences in isotope abundance ratios. *Rev Sci Instrum*. 1950;21(8):724-730. doi:10.1063/1.1745698
23. Craig H. Isotopic standards for carbon and oxygen and correction factors for mass-spectrometric analysis of carbon dioxide. *Geochim Cosmochim Acta*. 1957;12(1-2):133-149. doi:10.1016/0016-7037(57)90024-8
24. Baertschi P. Absolute ^{18}O content standard mean ocean water. *Earth Planet Sci Lett*. 1976;31(3):341-344. doi:10.1016/0012-821X(76)90115-1
25. Barkan E, Luz B. High precision measurements of $^{17}O/^{16}O$ and $^{18}O/^{16}O$ ratios in H_2O. *Rapid Commun Mass Spectrom*. 2005;19(24):3737-3742. doi:10.1002/rcm.2250
26. Lin Y, Clayton RN, Gröning M. Calibration of $\delta^{17}O$ and $\delta^{18}O$ of international measurement standards–VSMOW, VSMOW2, SLAP, and SLAP2. *Rapid Commun Mass Spectrom*. 2010;24(6):773-776. doi:10.1002/rcm.4449
27. Clayton RN, Grossman L, Mayeda TK. A component of primitive nuclear composition in carbonaceous meteorites. *Science*. 1973;182(4111):485-488. doi:10.1126/science.182.4111.485
28. Clayton RN, Mayeda TK. The oxygen isotope record in Murchison and other carbonaceous chondrites. *Earth Planet Sci Lett*. 1984;67(2):151-161. doi:10.1016/0012-821X(84)90110-9
29. Clayton RN, Mayeda TK. Oxygen isotopes in eucrites, shergottites, nakhlites, and chassignites. *Earth Planet Sci Lett*. 1983;62(1):1-6. doi:10.1016/0012-821X(83)90066-3
30. Fitzsimons ICW, Harte B, Clark RM. SIMS stable isotope measurement: counting statistics and analytical precision. *Mineral Mag*. 2000;64(1):59-83. doi:10.1180/002646100549139
31. Ireland T. R., Sapah M., Ávila J. N., Holden P., and Lanc P. 2014b. High-precision oxygen-isotope measurements with SHRIMP SI. National Institute of polar research, proceedings of the 5th symposium on polar science.
32. Tanaka R, Nakamura E. Determination of 17O-excess of terrestrial silicate/oxide minerals with respect to Vienna standard mean ocean

water (VSMOW). *Rapid Commun Mass Spectrom*. 2013;27(2):285-297. doi:10.1002/rcm.6453
33. Pack A, Tanaka R, Hering M, Sengupta S, Peters S, Nakamura E. The oxygen isotope composition of San Carlos olivine on the VSMOW2-SLAP2 scale. *Rapid Commun Mass Spectrom*. 2016;30(13):1495-1504. doi:10.1002/rcm.7582
34. Sharp ZD, Wostbrock JAG, Pack A. Mass-dependent triple oxygen isotope variations in terrestrial materials. *Geochem Perspect Lett*. 2018;7:27-31. doi:10.7185/geochemlet.1815
35. Hartley ME, Thordarson T, Taylor C, Fitton JG, EIMF. Evaluation of the effects of composition on instrumental mass fractionation during SIMS oxygen isotope analyses of glasses. *Chem Geol*. 2012;334:312-323. doi:10.1016/j.chemgeo.2012.10.027
36. Hartley ME, Thordarson T, Fitton JG, EIMF. Oxygen isotopes in melt inclusions and glasses from the Askja volcanic system, North Iceland. *Geochim Cosmochim Acta*. 2013;123:55-73. doi:10.1016/j.gca.2013.09.008
37. Manzini M, Bouvier AS, Baumgartner LP, Rose-Koga EF, Schiano P, Shimizu N. Grain scale processes recorded by oxygen isotopes in olivine-hosted melt inclusions from two MORB samples. *Chem Geol*. 2019;511:11-20. doi:10.1016/j.chemgeo.2019.02.025
38. Cooper AF, Ireland TR. Cretaceous sedimentation and metamorphism of the western Alpine schist protoliths associated with the pounamu ultramafic belt, Westland, New Zealand. *N Zeal J Geol Geophys*. 2013;56(4):188-199. doi:10.1080/00288306.2013.809776
39. Cooper AF, Ireland TR. The pounamu terrane, a new cretaceous exotic terrane within the Alpine schist, New Zealand, tectonically emplaced, deformed and metamorphosed during collision of the LIP Hikurangi plateau with Zealandia. *Gondw Res*. 2015;27(3):1266-1269. doi:10.1016/j.gr.2013.11.011
40. Peters ST, Alibabaie N, Pack A, et al. Triple oxygen isotope variations in magnetite from iron-oxide deposits, Central Iran, record magmatic fluid interaction with evaporite and carbonate host rocks. *Geology*. 2020;48(3):211-215. doi:10.1130/G46981.1
41. Vielzeuf D, Champenois M, Valley JW, Brunet F, Devidal JL. SIMS analyses of oxygen isotopes: matrix effects in Fe–mg–ca garnets. *Chem Geol*. 2005;223(4):208-226. doi:10.1016/j.chemgeo.2005.07.008
42. McKibbin SJ, Ireland TR, Amelin Y, O'Neill HSC, Holden P. Mn–Cr relative sensitivity factors for secondary ion mass spectrometry analysis of mg–Fe–ca olivine and implications for the Mn–Cr chronology of meteorites. *Geochim Cosmochim Acta*. 2013;110:216-228. doi:10.1016/j.gca.2013.02.025
43. McKibbin SJ, Ireland TR, Amelin Y, Holden P. Mn–Cr dating of Fe-and ca-rich olivine from 'quenched'and 'plutonic'angrite meteorites using secondary ion mass spectrometry. *Geochim Cosmochim Acta*. 2015;157:13-27. doi:10.1016/j.gca.2015.02.019
44. Taylor S, Herzog GF, Delaney JS. Crumbs from the crust of Vesta: achondritic cosmic spherules from the south pole water well. *Meteorit Planet Sci*. 2007;42(2):223-233. doi:10.1111/j.1945-5100.2007.tb00229.x
45. Goodrich CA, Delaney JS. Fe/mg-Fe/Mn relations of meteorites and primary heterogeneity of primitive achondrite parent bodies. *Geochim Cosmochim Acta*. 2000;64(1):149-160. doi:10.1016/S0016-7037(99)00107-6
46. Cordier C, Folco L, Suavet C, Sonzogni C, Rochette P. Major, trace element and oxygen isotope study of glass cosmic spherules of chondritic composition: the record of their source material and atmospheric entry heating. *Geochim Cosmochim Acta*. 2011;75(18):5203-5218. doi:10.1016/j.gca.2011.06.014
47. Cordier C, Suavet C, Folco L, Rochette P, Sonzogni C. HED-like cosmic spherules from the Transantarctic Mountains, Antarctica: major and trace element abundances and oxygen isotopic compositions. *Geochim Cosmochim Acta*. 2012;77:515-529. doi:10.1016/j.gca.2011.10.021
48. Greenwood RC, Burbine TH, Miller MF, Franchi IA. Melting and differentiation of early-formed asteroids: the perspective from high precision oxygen isotope studies. *Geochemistry*. 2017;77(1):1-43. doi:10.1016/j.chemer.2016.09.005
49. Greenwood RC, Burbine TH, Franchi IA. Linking asteroids and meteorites to the primordial planetesimal population. *Geochim Cosmochim Acta*. 2020;277:377-406. doi:10.1016/j.gca.2020.02.004
50. Thiemens M, Jackson T, Zipf E, Erdman PW, Van Egmond C. Carbon dioxide and oxygen isotope anomalies in the mesosphere and stratosphere. *Science*. 1995;270(5238):969-972. doi:10.1126/science.270.5238.969
51. Suavet C, Cordier C, Rochette P, et al. Ordinary chondrite related giant (>800 μm) cosmic spherules from the Transantarctic Mountains. *Antarctica Geochim Cosmochim Acta*. 2011a;75(20):6200-6210. doi:10.1016/j.gca.2011.07.034
52. Kita NT, Nagahara H, Tachibana S, et al. High precision SIMS oxygen three isotope study of chondrules in LL3 chondrites: role of ambient gas during chondrule formation. *Geochim Cosmochim Acta*. 2010;74(22):6610-6635. doi:10.1016/j.gca.2010.08.011
53. Jogo K, Nagashima K, Hutcheon ID, Krot AN, Nakamura T. Heavily metamorphosed clasts from the CV chondrite breccias Mokoia and Yamato-86009. *Meteorit Planet Sci*. 2012;47(12):2251-2268. doi:10.1111/maps.12042
54. Gurenko AA, Bindeman IN, Chaussidon M. Oxygen isotope heterogeneity of the mantle beneath the Canary Islands: insights from olivine phenocrysts. *Contrib Mineral Petrol*. 2011;162(2):349-363. doi:10.1007/s00410-010-0600-5
55. Gurenko AA, Chaussidon M. Oxygen isotope variations in primitive tholeiites of Iceland: evidence from a SIMS study of glass inclusions, olivine phenocrysts and pillow rim glasses. *Earth Planet Sci Lett*. 2002;205(1-2):63-79. doi:10.1016/S0012-821X(02)01005-1
56. Chaussidon M, Libourel G, Krot AN. Oxygen isotopic constraints on the origin of magnesian chondrules and on the gaseous reservoirs in the early solar system. *Geochim Cosmochim Acta*. 2008;72(7):1924-1938. doi:10.1016/j.gca.2008.01.015
57. Jochum KP, Nohl U. Reference materials in geochemistry and environmental research and the GeoReM database. *Chem Geol*. 2008;253(1–2):50-53. doi:10.1016/j.chemgeo.2008.04.002
58. Jochum KP, Stoll B. Reference materials for elemental and isotopic analyses by LA-(MC)-ICP–MS: successes and outstanding needs. In: *Sylvester, P (Ed), Laser Ablation ICP-MS in the Earth Sciences: Current Practices and Outstanding Issues*. Vol.40. Mineral Assoc Canada Short Course; 2008:147-168.
59. Valley JW, Graham CM. Ion microprobe analysis of oxygen isotope ratios in granulite facies magnetites: diffusive exchange as a guide to cooling history. *Contrib Mineral Petrol*. 1991;109(1):38-52. doi:10.1007/BF00687199
60. Hervig RL, Williams P, Thomas RM, Schauer SN, Steele IM. Microanalysis of oxygen isotopes in insulators by secondary ion mass spectrometry. *Int J Mass Spectrom Ion Process*. 1992;120(1–2):45-63. doi:10.1016/0168-1176(92)80051-2
61. Lyon IC, Saxton JM, Cornah SJ. Isotopic fractionation during secondary ionisation mass spectrometry: crystallographic orientation effects in magnetite. *Int J Mass Spectrom Ion Process*. 1998;172(1–2):115-122. doi:10.1016/S0168-1176(97)00143-2
62. Huberty JM, Kita NT, Kozdon R, et al. Crystal orientation effects in $\delta^{18}O$ for magnetite and hematite by SIMS. *Chem Geol*. 2010;276(3–4):269-283. doi:10.1016/j.chemgeo.2010.06.012
63. Clayton RN, Mayeda TK, Brownlee DE. Oxygen isotopes in deep-sea spherules. *Earth Planet Sci Lett*. 1986;79(3-4):235-240. doi:10.1016/0012-821X(86)90181-0
64. Genge MJ, Suttle M, Van Ginneken M. Olivine settling in cosmic spherules during atmospheric deceleration: an indicator of the orbital eccentricity of interplanetary dust. *Geophys Res Lett*. 2016;43(20):10646-10653. doi:10.1002/2016GL070874

65. Genge MJ. An increased abundance of micrometeorites on earth owing to vesicular parachutes. *Geophys Res Lett*. 2017;44(4):1679-1686. doi:10.1002/2016GL072490
66. Gounelle M, Engrand C, Maurette M, Kurat G, McKeegan KD, Brandstätter F. Small Antarctic micrometeorites: a mineralogical and in situ oxygen isotopic study. *Meteorit Planet Sci*. 2005;40(6):917-932. doi:10.1111/j.1945-5100.2005.tb00163.x
67. Schmitz B, Farley KA, Goderis S, et al. An extraterrestrial trigger for the mid-Ordovician ice age: dust from the breakup of the L-chondrite parent body. *Sci Adv*. 2019;5(9):eaax4184. doi:10.1126/sciadv.aax4184

SUPPORTING INFORMATION

Additional supporting information can be found online in the Supporting Information section at the end of this article.

How to cite this article: McKibbin SJ, Ávila JN, Ireland TR, et al. Triple-oxygen isotopes of stony micrometeorites by secondary ion mass spectrometry (SIMS): Olivine, basaltic glass and iron oxide matrix effects for sensitive high-mass resolution ion microprobe-stable isotope (SHRIMP-SI). *Rapid Commun Mass Spectrom*. 2025;39(1):e9921. doi:10.1002/rcm.9921